Phenomenological quantum description of the ultrafast response of arrayed waveguide gratings

L. Grave de Peralta[a)]

Department of Physics, Texas Tech University, Lubbock, Texas 79409, USA

This work presents a detailed and quantitative quantum description of the ultrafast response of arrayed waveguide gratings (AWG) illuminated with relatively intense short pulses of light. This is achieved with no more mathematical or conceptual complexities than that required by a classical description. The presented approach is based on the phenomenological interpretation of the photon, that is, a photon is what produces a "click" in a photodetector. This phenomenological approach was combined with the application of Feynman's rules for describing interference and Bohr's correspondence principle, i.e., quantum theory should somehow converge in the limit with the classical description of the interference phenomena. This basic approach reveals that, in apparent opposition to wide-held beliefs, especially designed AWGs can be used to produce interference in conditions where the "which-path" information is available. © *2010 American Institute of Physics.* [doi:10.1063/1.3512860]

I. INTRODUCTION

Arrayed waveguide gratings (AWG) are integrated-optics devices commonly used in wave division multiplexing optical networks.[1] AWGs are also suited for more advanced applications including super continuum filtering[2,3] and shaping ultrafast pulses of light.[4–6] This broad range of applications is the driving force behind the continuing interest in the design and function of these devices.[7–10] From a physics point of view, AWGs are wave-front-division-based spectrometers designed and fabricated for a basic function: to spectrally decompose the electromagnetic radiation incident in the input, resulting in light with different frequencies coming out of distinct outputs of the device.[11] This capability extends to the extreme case where an AWG is illuminated with pulses of light so short that pulses do not overlap at all in the common path of the spectrometer.[5,6] This physically interesting situation has been previously studied using classical approaches.[5,6,11] The author presents in this work, for the first time, a quantum description of the interference in AWGs illuminated with relatively intense ultrafast pulses of light. In these experiments[4–6] single photon events are not measured; however, it is interesting to analyze the experimental results, focusing the attention in the quantum nature of light. It is reasonable to attempt this analysis because, according to Bohr's correspondence principle,[12] classical optics should be an extreme instance of the more precise quantum description of light. A full quantum electrodynamics (QED) (Refs. 13 and 14) description of diffraction of ultra short pulses of light by an AWG would be unnecessarily complicated. Instead, the author presents a phenomenological but rigorous, quantum description based on the use of the most simple of the three common interpretations of the photon,[15] that is, a photon is what produces a "click" in a photodetector. In addition, Feynman's basic quantum rules for describing interference were used. These rules were summarized by Feynman as (1) the probability of an event is given by $p = |\Phi|^2$, where Φ is a complex number which is called probability amplitude and (2) when an event can occur in several alternative ways, the probability amplitude for the event is the (properly normalized to one) sum of the probability amplitudes for each way considered separately.[16] These basic ideas were chosen because this approach allows one to explore the classical limit of the quantum theory without more mathematical or conceptual complexities than that required by a classical description. Nevertheless, this basic phenomenological approach reveals that, in apparent opposition to wide-held beliefs, especially designed AWGs can be used for observing interference in conditions where the "which path" information is available.[17]

This paper is organized as follows: In Sec. II, a brief review of the classical description of the diffraction by a single rectangular slit is presented. Based on the classical results and the application of the correspondence principle, a phenomenological quantum description of the diffraction by a single rectangular slit is presented in Sec. III. In Sec. IV, a phenomenological quantum description of diffraction by a grating is worked out using the superposition principle; a generalization applicable to AWGs is presented in Sec. V. A brief discussion about the relation between interference and which-path information in a quantum description is made in Sec. VI, and the application of these ideas to the case of an AWG illuminated with ultrafast pulses of light is presented in Sec. VII. In Sec. VIII, the author discusses how the occurrence of interference, in an AWG illuminated with pulses of light so short that pulses do not overlap at all in the common path of the spectrometer, does not violate the uncertainty principle.[16] Finally, the conclusions of this work are given in Sec. IX.

II. CLASSICAL DESCRIPTION OF DIFFRACTION BY A SINGLE RECTANGULAR SLIT

Figure 1 shows the schematic of the transversal section of a typical experimental arrangement used to observe the

---

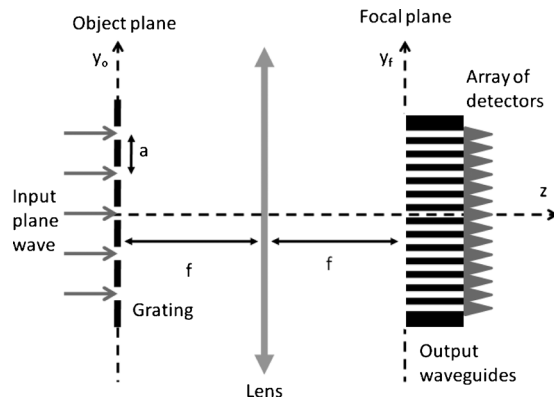a)Electronic mail: luis.grave-de-peralta@ttu.edu.

108, 103110-1

FIG. 1. Schematics of the transversal section of a typical experimental arrangement for observing diffraction by a grating.

diffraction of light by a multiple-slit. In this section it is supposed that all slits are closed except the central one. A two-dimensional (2D) array of output waveguides [see Fig. 2(a)], placed at the focal plane of a convergent lens with focal length (f), is used to collect the Fraunhofer diffraction pattern that corresponds to the rectangular slit placed at a distance f in front of the lens. A 2D array of photodetectors is coupled to the output waveguides to register and record the pattern. When the slit is illuminated by a monochromatic wave traveling in the z-axis direction, i.e., impinging perpendicularly to the object plane containing the slit, the time-averaged intensity (I) in the diffraction pattern collected at the focal plane is described by the following expressions:[18,19]

$$I(x_f,y_f) = \tfrac{1}{2}c\varepsilon_o|U(x_f,y_f)|^2, \tag{1}$$

with

$$U(x_f,y_f) = \tfrac{1}{i\lambda f}FT[U(x_o,y_o)]_{f_x\to(x_f/\lambda f),f_y\to(y_f/\lambda f)}, \tag{2}$$

and

$$FT[U(x_o,y_o)]_{f_x\to(x_f/\lambda f),f_y\to(y_f/\lambda f)}$$
$$= \int\int U(x_o,y_o)e^{-i(2\pi/\lambda f)(x_f x_o + y_f y_o)}dx_o dy_o, \tag{3}$$

where FT means 2D Fourier-transform, c is the speed of the light, ε_o and λ are the vacuum electrical permittivity and the wavelength of the light, respectively; i is the imaginary unit,
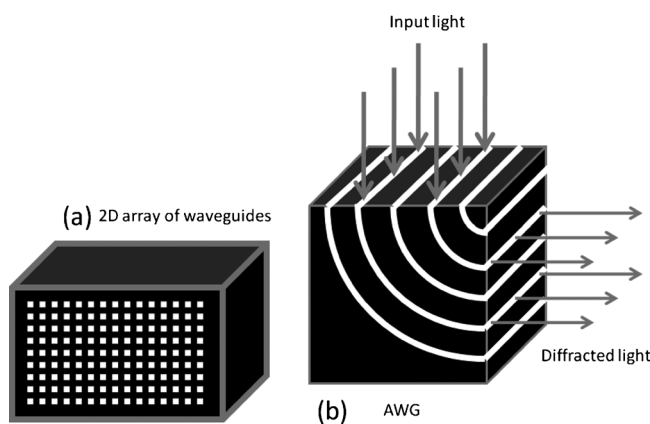

FIG. 2. Schematics of (a) a 2D array of waveguides and (b) a volume AWG.

the integration is over the object plane, and the subindices o and f refer to the object and focal planes, respectively. The optical disturbance $U(R)$ at a point R is a complex function. It is related to the amplitude of the electric field (E) by the following relation:[19]

$$E(R,t) = Re[U(R)e^{-i2\pi\nu t}], \tag{4}$$

where ν is the frequency of the light and Re is shorthand notation for *the real part of*. This discussion will consider light to be linearly polarized; thus, $E(R,t)$ can be described by a scalar harmonic function with amplitude equal to $|U|$. For a rectangular slit, the optical disturbance at the object plane is given by the following expression:[19]

$$U(x_0,y_0) = E_o\text{rect}\left(\frac{x_o}{L_x}\right)\text{rect}\left(\frac{y_o}{L_y}\right), \tag{5}$$

where E_o is the constant value of the amplitude of the electric field at the slit, and L_x and L_y are the width of the slit in the horizontal and vertical directions, respectively. The function $\text{rect}(\xi)$ and its Fourier-transform $\text{sinc}(f_\xi)$ are defined in Appendix A. Substituting (5) into (2) results:

$$U(x_f,y_f) = \frac{E_o L_x L_y}{i\lambda f}\text{sinc}\left(\frac{L_x}{\lambda f}x_f\right)\text{sinc}\left(\frac{L_y}{\lambda f}y_f\right). \tag{6}$$

Thus, the time-averaged intensity of the diffraction pattern is obtained by substituting (6) into (1):

$$I(x_f,y_f) = \frac{1}{2}c\varepsilon_o E_o^2\left[\left(\frac{L_x L_y}{\lambda f}\right)^2\text{sinc}^2\left(\frac{L_x}{\lambda f}x_f\right)\text{sinc}^2\left(\frac{L_y}{\lambda f}y_f\right)\right]. \tag{7}$$

A detailed discussion of the characteristics of the diffraction pattern described by expression (7) can be found everywhere.[18,19] The total electromagnetic power (P) arriving at the focal plane is given by the following integral:

$$P = \int\int I(x_f,y_f)dx_f dy_f. \tag{8}$$

Substituting (7) in (8) results in:

$$P = \left(\tfrac{1}{2}c\varepsilon_o E_o^2\right)L_x L_y. \tag{9}$$

The right term of expression (9) is the total electromagnetic power passing through the slit. As a consequence, as expected, the total power passing through the slit equals the total power reaching the focal plane. Assuming that the output waveguides have a core with an effective transversal area A_p of a few μm^2, and that there is a well designed experimental set up where smooth diffraction patterns are obtained, the intensity should have an approximately constant value along the core of any output waveguide in the 2D array. In this approximation, assuming no coupling losses and ideal photodetectors with 100% efficiency, the time-averaged power $P(x_f^j, y_f^k)$ collected by the waveguide (j,k) that is centered at the point (x_f^j, y_f^k), and registered in the photodetector (j,k), can be calculated as:

$$P(x_f^j,y_f^k) = \int\int_{wg(j,k)} I(x_f,y_f)dx_f dy_f \approx A_p I(x_f^j,y_f^k). \tag{10}$$

III. PHENOMENOLOGICAL QUANTUM DESCRIPTION OF DIFFRACTION BY A SINGLE RECTANGULAR SLIT

A quantum description of diffraction is required when the slit is illuminated with feeble light or single photons. In these experiments, the diffraction pattern is formed gradually in the object plane by the accumulation of numerous clicks, i.e., individual photon-detection events.[17] In a quantum picture, when the slit is uniformly illuminated with monochromatic light of frequency ν, the time-averaged power distribution registered by the array of detectors shown in Fig. 1 can be calculated using the following expression:

$$P(x_f^j, y_f^k) = Nh\nu p(x_f^j, y_f^k), \qquad (11)$$

where N is the average photon rate passing through the slit, h is Planck's constant, and $p(x_f^j, y_f^k)$ is the probability of the photon-detection event: the registration of the arrival of a photon (a click) at the (j,k)-detector, which is coupled to the output waveguide centered at the point (x_f^j, y_f^k) in the focal plane. Experimentally, $p(x_f^j, y_f^k)$ is determined by the fraction of the N photons, passing through the slit per unit of time, that are registered by the (j,k)-photodetector. Assuming no coupling losses and ideal photodetectors with 100% efficiency, N is also the average photon rate arriving at the 2D array of photodetectors. The quantum description of diffraction is based on the concept of probability amplitude.[16] Following Feynman's first rule, the probability $p(x_f^j, y_f^k)$ of collecting a photon at the waveguide (j,k) is given by the square of the absolute value of the probability amplitude $\Phi(x_f^j, y_f^k)$. A first principle calculation of Φ may be challenging. Fortunately, it is simpler in this case to invoke Bohr's correspondence principle.[12] Classical and quantum descriptions of diffraction by a rectangular slit should give equal results when the amplitude of the input plane wave is relatively large; i.e., when a large number of photons arrive at the focal plane. In the quantum picture, the time-averaged power distribution registered by the 2D array of photodetectors can be calculated using the following expression:

$$P(x_f^j, y_f^k) = Nh\nu |\Phi(x_f^j, y_f^k)|^2. \qquad (12)$$

It is useful to introduce an auxiliary function $\Omega(x_f, y_f)$, continuous in the variables x_f, y_f, and defined by the following relation:

$$\int\int_{wg(j,k)} |\Omega(x_f, y_f)|^2 dx_f dy_f \approx A_p |\Omega(x_f^j, y_f^k)|^2$$
$$= |\Phi(x_f^j, y_f^k)|^2, \qquad (13)$$

where the integration is over the transversal section of an output waveguide and Ω has dimensions of probability amplitude density (probability amplitude per unit of area). From (12) and (13) and comparing with (10) follows that:

$$I(x_f, y_f) = Nh\nu |\Omega(x_f, y_f)|^2. \qquad (14)$$

Expression (14) is formally similar to expression (1); however, unlike the classical optical disturbance U, the probability amplitude density Ω must be normalized to the unity:

$$\int\int |\Omega(x_f, y_f)|^2 dx_f dy_f = 1. \qquad (15)$$

Expression (15) states that if a photon passes through the slit, a click will be registered in some photodetector. Comparing expressions (14) and (7) and using Bohr's correspondence principle results:

$$\{Nh\nu\}|\Omega(x_f, y_f)|^2 = \left\{ \frac{1}{2} c\varepsilon_o E_o^2 L_x L_y \right\}$$
$$\times \left[\frac{L_x L_y}{(\lambda f)^2} \mathrm{sinc}^2\left(\frac{L_x}{\lambda f}x_f\right) \mathrm{sinc}^2\left(\frac{L_y}{\lambda f}y_f\right) \right]. \qquad (16)$$

From expression (9), the factors in curly brackets on both sides of (16) are equal to the total power passing through the slit. As a consequence:

$$|\Omega(x_f, y_f)|^2 = \frac{L_x L_y}{(\lambda f)^2} \mathrm{sinc}^2\left(\frac{L_x}{\lambda f}x_f\right) \mathrm{sinc}^2\left(\frac{L_y}{\lambda f}y_f\right). \qquad (17)$$

Knowing $|\Omega|^2$, one can use Feynman's first rule and expressions (11)–(13) to find that the probability of collecting a photon in the waveguide (j,k) is given by the following expression:

$$p(x_f^j, y_f^k) = \frac{A_p L_x L_y}{(\lambda f)^2} \mathrm{sinc}^2\left(\frac{L_x}{\lambda f}x_f^j\right) \mathrm{sinc}^2\left(\frac{L_y}{\lambda f}y_f^k\right) \qquad (18)$$

Expression (17) determines Ω except for an arbitrary phase factor. Using a value of zero results:

$$\Omega(x_f, y_f) = \frac{\sqrt{L_x L_y}}{\lambda f} \mathrm{sinc}\left(\frac{L_x}{\lambda f}x_f\right) \mathrm{sinc}\left(\frac{L_y}{\lambda f}y_f\right). \qquad (19)$$

As expected, Ω is completely determined by the geometry of the slit-lens arrangement and the wavelength of the light. Ω given by (19) satisfies the normalization condition (15). A direct comparison of (19) and (6) allows one to obtain the following relation between the quantum probability amplitude density $\Omega(x_f, y_f)$ and the values of the classical optical disturbance $U(x_f, y_f)$ in the focal plane:

$$\Omega(x_f, y_f) = \beta U(x_f, y_f), \qquad (20)$$

where β is the dimensional constant:

$$\beta = \frac{i}{E_o \sqrt{L_x L_y}}. \qquad (21)$$

Relation (20) states that, in the classical limit, the probability amplitude per unit area of registering a click at the point (x_f, y_f) in the focal plane of the experimental set up (shown in Fig. 1) is directly proportional to the optical disturbance value at that point. This provides a way to calculate the probability distribution of clicks in the 2D array of photodetectors in the classical limit, without having to rely on the mathematical subtleness of more elaborated quantum theories of photons.[13–15] In this sense, satisfying relation (20) can be seen as a mandatory test for any successful quantum theory of photons. Expressions (11)–(13) provide a phenomenological definition of Ω. It is worth noting that this definition does not identify the distribution of probability amplitude densi-

ties $\Omega(x_f, y_f)$ as the values resulting from evaluating some quantum field or quantum wave function $\Psi(x, y, z)$ at the focal plane. Independent from the existence or nonexistence of a photon wave function,[15,20] and independent from the formulation of the quantum field theory,[13,14] calculated values of Ω using any quantum theory of photons (in the classical limit) should match the values of Ω calculated using expression (20). The probability distribution given by (18) is stationary because the incident light is monochromatic, i.e., all photons have the same energy $h\nu$. Expression (4) shows the temporal dependence of the optical disturbance. Consequently, in the case of monochromatic illumination, the temporal dependence of the probability amplitude density is given by the following expression:

$$\Omega_\nu(x_f, y_f, t) = \Omega(x_f, y_f)e^{-i2\pi\nu t}. \tag{22}$$

IV. PHENOMENOLOGICAL QUANTUM DESCRIPTION OF DIFFRACTION BY A GRATING

The quantum description of the diffraction by a grating with $M+1$ rectangular slits and period a (see Fig. 1) can be done in terms of probability amplitudes using the superposition principle contained in Feynman's second rule.[16] Assuming uniform illumination of the grating, a photon has an equal probability $[1/(M+1)]$ to pass through any of the slits. Consequently, the probability amplitude density (properly normalized to one) of registering a photon in the focal plane at the point (x_f, y_f) after passing through the multiple-slit is given by the following expression:

$$\Omega_g(x_f, y_f) = \frac{1}{\sqrt{M+1}}\left\{ \Omega(x_f, y_f) + \sum_{k=1}^{M/2} [\Omega_{+k}(x_f, y_f) + \Omega_{-k}(x_f, y_f)] \right\}, \tag{23}$$

where $\Omega_{\pm k}$ is the probability amplitude density of registering a photon at point (x_f, y_f) in the focal plane after passing through the kth slit of the top $(+)$ or bottom $(-)$ half of the grating. The simplest way to find the expressions describing these probability amplitude densities is to calculate the corresponding classical optical disturbances U_{+k} and U_{-k}, and then use relation (20). Each slit is shifted by $\pm ka$ in respect to the central one; thus:

$$U_{\pm k}(x_0, y_0) = U(x_0, y_0 \pm ka). \tag{24}$$

As a consequence, substituting (24) into (2), using the shift property of the Fourier-transform,[19] and then using (20) results in:

$$\Omega_{\pm k}(x_f, y_f) = \Omega(x_f, y_f)e^{\pm i(2\pi/\lambda f)y_f ka}. \tag{25}$$

Expression (25) permits one to rewrite (23) in the following way:

$$\Omega_g(x_f, y_f) = \frac{1}{\sqrt{M+1}}\Omega(x_f, y_f)\Sigma(y_f), \tag{26}$$

where

$$\Sigma(y_f) = 1 + \sum_{k=1}^{M/2} [e^{+i2k\alpha} + e^{-i2k\alpha}], \quad \alpha = \frac{\pi}{\lambda f}y_f a. \tag{27}$$

As shown in Appendix B, the sum in expression (27) can be evaluated exactly. This results in a simple expression for Ω_g:

$$\Omega_g(x_f, y_f) = \frac{1}{\sqrt{M+1}}\Omega(x_f, y_f)g(y_f), \tag{28}$$

with

$$g(y_f) = \frac{\sin[(M+1)\alpha]}{\sin\alpha}. \tag{29}$$

The total photon rate through the grating is $(M+1)N$; thus, substituting N by $(M+1)N$ and Ω by Ω_g in expression (14) allows one to obtain the time-averaged intensity distribution, at the focal plane, corresponding to a grating illuminated by a relatively intense input beam:

$$I_g(x_f, y_f) = Nh\nu|\Omega(x_f, y_f)|^2 g^2(y_f). \tag{30}$$

In expression (30), the last factor corresponds to the interference associated with the superposition of $M+1$ probability amplitude densities. Using the following property:[18]

$$\lim_{\alpha \to m\pi} \frac{\sin[(M+1)\alpha]}{\sin(\alpha)} = \pm(M+1),$$

$$m = 0, \pm 1, \pm 2, \dots . \tag{31}$$

The positions of the interference maxima are given by the following expression:[18]

$$\alpha = m\pi \Rightarrow y_f = m\frac{\lambda f}{a}, \quad m = 0, \pm 1, \pm 2, \dots . \tag{32}$$

In addition, a comparison of (30) and (14) reveals that a grating produces interference maxima $(M+1)^2$ times more intense than the intensity maximum in a single slit diffraction pattern.[18] Knowing $|\Omega_g|^2$, one can use Feynman's first rule and expressions (11)–(13) to find that the probability distribution corresponding to expression (30) is given by the following expression:

$$p_g(x_f^j, y_f^k) = \frac{A_p L_x L_y}{(M+1)(\lambda f)^2}\text{sinc}^2\left(\frac{L_x}{\lambda f}x_f^j\right)\text{sinc}^2\left(\frac{L_y}{\lambda f}y_f^k\right)$$

$$\times \frac{\sin^2[(M+1)\alpha]}{\sin^2\alpha}. \tag{33}$$

Expression (33) reduces to (18) for $M=0$. Like the probability distribution given by (18), p_g is stationary because the incident light is monochromatic, i.e., all photons have the same energy $h\nu$. As a consequence, the temporal dependence of the probability amplitude density is given by the following expression:

$$\Omega_{g\nu}(x_f, y_f, t) = \Omega_g(x_f, y_f)e^{-i2\pi\nu t}. \tag{34}$$

It is worth noting that the probability distribution described by expression (33), which was obtained in the classical limit of a quantum description, is still valid when the multiple-slit is illuminated with feeble light or single photons.[17] This is in agreement with the absence of N in expression (33) and with
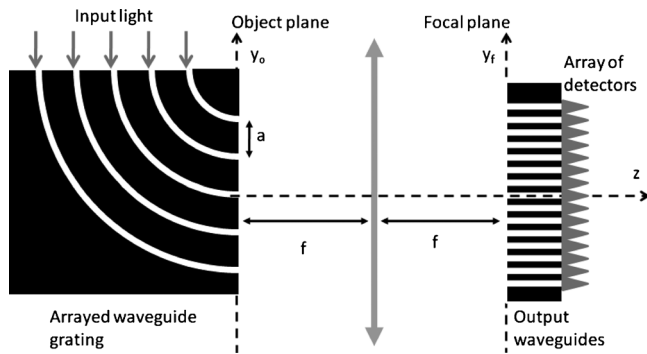
FIG. 3. Schematics of the transversal section of an experimental arrangement for observing diffraction by an AWG.

the famous Dirac's dictum: "each photon then interferes only with itself."[21,22]

V. PHENOMENOLOGICAL QUANTUM DESCRIPTION OF DIFFRACTION BY AN AWG

Gratings are often used in spectroscopy applications because the position of the interference maxima when $m \neq 0$ depends on the frequency of the illuminating light. However, a bright zero-order diffraction is always formed in the center of the diffraction pattern ($y_f = 0$) independent of the light frequency. This sometimes undesirable feature can be avoided by using an AWG.[1] Figure 2(b) shows a schematic of a volume AWG formed by a set of curved slab waveguides. When the input face of the AWG is illuminated by a plane wave, light is coupled uniformly to the set of slab waveguides and radiated through the output face of the AWG, which is basically a grating formed by $M+1$ rectangular slits. However, unlike common gratings, there is phase difference between light emitted by consecutive output slits equal to:

$$\Delta\varphi = 2\pi\frac{\Delta L}{\lambda/n},\tag{35}$$

where n is the effective refractive index of the slab waveguide and $n\Delta L$ is the optical path length difference between consecutive slab waveguides. AWGs are designed to produce a diffraction pattern where the m_d-order interference maximum ($m_d \gg 1$) appears at the center of the pattern when the AWG is illuminated with light of wavelength λ_o. This is achieved when ΔL is given by the following expression:[1]

$$\Delta L = m_d\frac{\lambda_o}{n}.\tag{36}$$

By using (35) and (36) can be rewritten in the following way:

$$\Delta\varphi = 2\pi m_d\frac{\lambda_o}{\lambda} = 2\pi m_d\frac{\nu}{\nu_o}.\tag{37}$$

Figure 3 shows the schematic of the transversal section of an experimental arrangement used to observe the diffraction of light by an AWG. The quantum description of the diffraction by an AWG with $M+1$ slab waveguides can be done by following the same steps described in Sec. IV. In order to include the phase shift given by expression (37), expression

(24) should be modified in the following way:[5,6]

$$U_{\pm k}(x_0,y_0) = U(x_0,y_0 \pm ka)e^{-i2\pi km_d(\nu/\nu_o)}.\tag{38}$$

Expression (38) assumes that for the design frequency ($\nu_o = \lambda_o/c$) the phase of the optical disturbance is equal to zero in the middle waveguide of the grating ($k=0$). The phase changes by $\Delta\varphi$ from one waveguide to the next. Now, substituting (38) in (2), using the linearity and shift properties of the Fourier-transform,[19] and then using (20) results in:

$$\Omega_{\pm k}(x_f,y_f,\nu) = \Omega(x_f,y_f)e^{\pm i(2\pi/\lambda f)y_f k(a+m_d(\lambda f/y_f)(\nu/\nu_o))}.\tag{39}$$

Substituting (39) into (23) results in (26) and (27) but now with:

$$\alpha = \alpha_\nu = \frac{\pi}{\lambda f}y_f\left(a + m_d\frac{\lambda f}{y_f}\frac{\nu}{\nu_o}\right).\tag{40}$$

Consequently, expressions (28)–(30), (33), and (34) are still valid for AWGs after substituting α by α_ν. For $m_d = 0$, α given by (40) reduces to its value in (27). This is in agreement with the fact that an AWG with $\Delta L = 0$ produces the same diffraction pattern that a common grating does. For AWGs, the positions of the interference maxima are given by the following expression:

$$\alpha_\nu = m\pi \Rightarrow y_f = \left(m - m_d\frac{\nu}{\nu_o}\right)\frac{\lambda f}{a},$$

$$m = m_d, m_d \pm 1, m_d \pm 2, \ldots.\tag{41}$$

Well designed AWGs work in the $m = m_d$ diffraction order. In this case, for $\nu = \nu_o$, $y_f = 0$, i.e., the design frequency is collected at the center of the AWG interference pattern. The useful spectral range of an AWG is determined by its free spectral range (FSR):[1,4–6]

$$FSR = \frac{c/n}{\Delta L} = \frac{\nu_o}{m_d}.\tag{42}$$

This means that if the AWG is illuminated with light of different frequencies, an interference maximum will be formed at $y_f = 0$ for all the frequencies that differ from the design frequency by a multiple of FSR. This property can be easily confirmed using (41) and (42). AWGs are used in spectroscopy applications because simultaneous illumination with several input frequencies in the range $\nu_o - FSR/2 < \nu < \nu_o + FSR/2$ results in several interference maxima spatially spread in the spatial range $-\lambda f/2a < y_f < \lambda f/2a$ at the object plane.

VI. INTERFERENCE AND WHICH-PATH INFORMATION

The dependencies on y_f^k of two different probability distributions, calculated using expressions (33) and (40) for $x_f^j = 0$, are plotted in Fig. 4. The parameter values used were $A_p = 25$ μm^2, $L_y = 5$ μm, $\lambda = \lambda_o = 1.56$ μm, $a = 20$ μm, $f = 3$ mm, and $m_d = 3876$. These parameter values match the parameters of the especially designed AWG used in previously published experiments.[5,6,11] This allows one to compare the simulation results presented in this work with real experimental data. The discontinuous curve in Fig. 4 corresponds to the diffraction by a single slit ($M=0$). In this case,
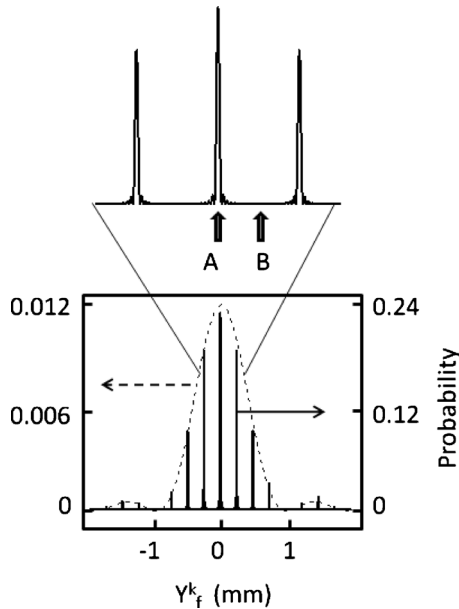
FIG. 4. Dependence on y_f^k of the calculated probabilities for $x_f^j=0$. Diffraction by (a) a single slit ($M=0$, discontinuous line) and (b) 21 slits ($M=20$, continuous line). Inset: A and B indicate the positions of two detectors.

the probability distribution exhibits a broad central peak. Inside of the central peak, $p(x_f^j=0,y_f^k)$ decreases smoothly and monotonically from the center of the diffraction pattern to the first diffraction minima at $|y_f^k| \sim 1$ mm. The continuous curve in Fig. 4 corresponds to the diffraction by an AWG with 21 slab waveguides ($M=20$). Seven well-defined peaks are observed in the same region occupied by the broad central peak of the discontinuous curve. These peaks are signature features of interference because they cannot be obtained by adding several single slit diffraction patterns. If all the slab waveguides of the AWG except the central one were obstructed, every incoming photon would leave the AWG through the central slit. The diffraction pattern at the focal plane would correspond to the diffraction by a single slit, which lacks the signature features of interference. In contrast, if all the slab waveguides of the AWG were open, interference fringes would be clearly observed in the diffraction pattern. In AWGs, photons traversing distinct waveguides of the grating take different times to arrive at the 2D array of detectors; thus, one could think that measuring the time of flight of the photons could reveal which path a photon took. However, this is not possible in experiments where an AWG is illuminated with monochromatic light because a simple harmonic wave is extremely long and featureless. The absence of temporally distinguishable features in the input wave impedes determining whether the click that occurred at time t_c in the photodetector (j,k) was produced, for instance, by a photon that entered at time t_1 in the AWG and traversed the AWG through the shortest waveguide, or by another photon that entered at time $t_2 < t_1$ in the AWG and traversed the AWG through the longest waveguide. It is common in specialized quantum mechanics literature to summarize these facts as follows: "a perfect interference pattern (equally energetic photons arrive in specific places at the focal plane) arises only when there is no possible way of

finding out which path the particle took."[17] Due to practical reasons, two-path experimental arrangements are often used in interference experiments with monochromatic feeble light. Instead of an AWG, double-slit[23,24] or Mach–Zehnder interferometer arrangements[17,25,26] are commonly used as the two-path arrangements. In addition, the 2D array of photodetectors is often substituted by a single photodetector. The single photodetector is either translated through the area covered by the diffraction pattern,[23,24] or the path length of one arm of the interferometer is changed.[25,26] Occurrence of interference is often established when the measured probability distribution of clicks contains the characteristic spatial features of interference. It is implicit in the summary-phrase cited above that the photodetectors are adequate for registering the perfect interference pattern that arises when there is no possible way of finding out which path the particle took. This means that photodetectors or scanning step sizes should be small enough to resolve the interference fringes. The width of the peaks in the continuous curve in Fig. 4 decreases when the number of different optical paths in the experimental arrangement increases.[18,19] In order to resolve these peaks, photodetectors or scanning step sizes should be much smaller than the width of the peaks. Evidently, this requirement is easier to achieve in two-path experimental arrangements. A second consideration about the photodetectors is that they should not be the reason why perfect interference patterns occur. Assuming that the parameters of the photodetector arrangement have been well chosen, when all slab waveguides are open the measured probability distribution of clicks at the focal plane should be similar to the continuous curve in Fig. 4. However, when all slab waveguides except the central one are obstructed, the distribution should be similar to the discontinuous curve in Fig. 4. This means that in absence of propagation losses in the hypothetical experimental arrangement show in Fig. 3, the measured probability distribution of clicks should be independent of the length of the output waveguides, i.e., the number and energy of the photons that enter any output waveguide should be equal to that of the ones that make the corresponding detector to click. It is also implicit in the summary-phrase cited above that the "possible ways of finding out which path the particle took" include the possibility of knowing, even without actual experimental confirmation, which path the photon responsible for a particular click took.[25,26] A possible way to acquire this knowledge could be by replacing the photodetector with another measurement device that does not disturb the original experiment[25] but does reveal the which-path information. For instance, a free-space auto-correlation apparatus may be used to try to determine time of flight values.[5,6] If the which-path information is obtained using such a device, then one should expect that no interference pattern will arise when the experiment is repeated with the original photodetector. In the opposite case, if it was impossible to obtain the which-path information, one should expect that a perfect interference pattern will arise in the original arrangement. It is worth noting that only two static detectors are enough to distinguish between the cases $M=0$ and $M \gg 1$. The inset in Fig. 4 shows a possible arrangement of two photodetectors designed to distinguish

between the two cases using a source that emits light with the design frequency ν_o. Photodetector A is placed at the central point of the diffraction pattern. Photodetector B is placed horizontally at $x_f^j = 0$ and vertically at the midpoint between the $m = m_d$ and $m = m_d + 1$ interference maxima ($y_f^k = \lambda f / 2a$). If all the slab waveguides of the AWG except the central one were obstructed, then both photodetectors would register a similar number of clicks ($A_1 \sim B_1/2$). However, if all the $M+1$ slab waveguides of the AWG were open, photodetector A would count a much larger number of clicks than photodetector B($A_{M+1} > A_1 \gg B_{M+1} \ll B_1$). In addition, the average number of clicks registered by the photodetectors would be time-independent due to the stationary character of the probability distribution (33). If the frequency of the input light was not ν_o, it would be necessary to change the locations of the two photodetectors because the diffraction pattern would shift vertically with respect to the one corresponding to $\nu = \nu_o$. For instance, for $\nu = \nu_o + FSR/2$, an interference maximum (minimum) would form in the position of the photodetector B (A). As a consequence, if the photodetectors were not switched, the relation between their measurements would be $B_{M+1} > B_1 \gg A_{M+1} \ll A_1$. It is of particular importance to note that this method of interference recognition is appropriate for experiment using monochromatic or narrow band light. However, this method is not appropriate for experiments using a broad band source of light because minima of interference corresponding to a particular frequency may be masked by maxima of interference corresponding to another frequency. This problem is particularly acute in two-path experimental arrangements, where the spatial interference fringes are relatively broad when compared with those in multiple-path based experiments.

There is an alternative method for demonstrating the occurrence of multiple-slit interference. As it will become clear in Sec. VI, this second method is well-suited for experiments with broad band illumination. The method consists of substituting photodetectors A and B with two spectrometers. In addition, the AWG should be illuminated successively using two monochromatic light sources that have two different, adequately chosen, frequencies. For instance (using the experimental set up shown in Fig. 3, with the spectrometers A and B placed as shown in the insert in Fig. 4) if only the central slab waveguide was open and the AWG was successively illuminated by monochromatic light with frequencies $\nu_1 = \nu_o$ and $\nu_2 = \nu_o + FSR/2$, then both spectrometers would register the successive arrival of photons having energies equal to $h\nu_1$ and $h\nu_2$. However, if all the slab waveguides were open, spectrometer A would only register the arrival of photons with energy $h\nu_1$ while spectrometer B would only register the arrival of photons with energy $h\nu_2$. It has been assumed in these arguments, implicitly, that measured spectra in A and B have at most a single narrow peak each, and that a spectral shift can be observed by comparing the spectral position of the peaks, i.e.,:

$$\Delta \nu_{peack} \ll FSR/2, \tag{43}$$

where $\Delta \nu_{\text{peack}}$ is the width of the peaks. The temporal dependence of the optical signal, which comes out from the AWG and arrives at the external spectrometer, can be obtained

from the measured spectrum with a simple Fourier transform operation.[4–6] The Fourier transform of a single narrow peak is a single long pulse of duration Δt_{sp}, given by the following expression:

$$\Delta t_{sp} \approx 1/\Delta \nu_{peack} \gg 2/FST = 2\Delta t, \tag{44}$$

where Δt is the time delay corresponding to the difference in optical path between consecutive slab waveguides of the AWG:[4–6]

$$\Delta t = \frac{\Delta L}{c/n} = \frac{1}{FSR}. \tag{45}$$

The lack of internal structure in the single long pulse impedes to determine which slit photons arriving at the external spectrometer passed through. Consequently, one can rephrase the common saying about the relation between interference and which-path information in the following way: a perfect interference pattern (photons with different energies arrive in distinct specific places at the focal plane) arises only when there is no possible way of finding out which path the photon took. It is implicit in this rephrasing that the spectrometers permit one to recognize that photons with different energies arrive in distinct specific places at the focal plane. This means that (1) the resolution of the spectrometers should be enough to resolve the peaks in the measured spectra and (2) the chosen spectrometers should not be the reason why a perfect interference pattern arises. That is, assuming that the parameters of the spectrometers have been well chosen, when all the slab waveguides except the central one are obstructed, spectra measured at positions A and B should be similar to each other. However, when all slab waveguides are open, a spectral shift would be observed when comparing the spectral position of the peaks corresponding to spectra measured at positions A and B.

Summarizing this section, there are two different methods for recognizing when interference occurs. The first one, commonly used in experiments with monochromatic feeble light,[23–26] involves photodetectors to determine, experimentally, that equally energetic photons arrive in specific places at the focal plane. In these experiments, spatial interference fringes are recorded. This method is not appropriate for experiments using a broad band source of light because the spatial interference features may be smeared out due to the spatial coincidence of minima of interference corresponding to a particular frequency with the maxima of interference corresponding to another frequency. The absence of spatial "wiggles" may be erroneously interpreted as the absence of interference. The second method involves using at least two spectrometers to record the output spectra corresponding to input illumination with at least two different frequencies. Using the second method, the occurrence of interference is recognized by determining that photons with different energies arrive in distinct specific places at the focal plane. This spectral method for identifying the occurrence of interference is appropriate for experiments with pulsed light. No matter what method is used, the external instrument used to identify the occurrence of interference should (1) be able to resolve the interference features and (2) not be the reason why interference occurs. There is a wide-held belief that can be sum-

marized as follows: *interference features are present in the recorded data only when there is no possible way of finding out which path the photon took.* This belief extends to the point that interference features should disappear as soon as one knows, even without actual experimental confirmation, the path of the photon responsible for a particular click. As it will be shown in Sec. VI, this belief is only justified in the context of interference experiments using monochromatic or narrow band light. In these experiments photodetectors are used and the interference features are spatial interference fringes.

VII. OBSERVING INTERFERENCE WHILE KNOWING WHICH SLIT PHOTONS PASSED THROUGH

In apparent opposition to wide-held beliefs regarding the relation between interference and which-path information, illuminating a especially designed AWG with a proper mode-locked laser allows one to produce interference in conditions where the which-path information is available.[5,6,11] If the laser emits a periodic sequence of relatively intense short pulses, such that the separation between consecutive pulses Δt_R is long enough, i.e.,:

$$\Delta t_R \gg (M+1)\Delta t. \tag{46}$$

And if the pulses are short enough, i.e., the pulse width $\Delta\tau \ll \Delta t$, then the AWG will generate a train of $M+1$ well separated pulse-replicas for each input pulse.[4–6] Pulse-replicas have the same spectral composition as the input pulse has but they have lower intensity. Obviously, all the photons forming the first (last) pulse-replica passed through the shortest (longer) slab waveguide; thus, when a proper mode-locked laser is used as the illumination source, it is, at least in principle, possible to know which slab waveguide photons passed through. Nevertheless, as it will be discussed below, interference also arises in these conditions, and photons with a definite energy are only collected in specific output waveguides in the experimental arrangement shown in Fig. 3. Let's assume for simplicity in this discussion, that the length of the pulses is bandwidth-limited, and that pulses are formed by a superposition of $Q+1$ monochromatic spectral components, all with the same intensity and with the following frequencies centered at the AWG design frequency ν_o:

$$\nu_l = \nu_o + \sigma_l, \quad \sigma_l = l\frac{FSR}{q}, \quad l = 0, \pm 1, \ldots, \pm Q/2, \tag{47}$$

where $q < Q$. Thus, the spectral width of the pulses is:

$$\Delta\nu = \frac{QFSR}{q} \sim \frac{1}{\Delta\tau}. \tag{48}$$

It follows from (45) and (48) that the temporal relation $\Delta\tau \ll \Delta t$ implies the spectral relation $\Delta\nu \gg FSR$. As discussed in Sec. V, the probability amplitude density $\Omega_{AWG,\nu}$ of collecting a photon with energy $h\nu_l$ at the time t in the point (x_f, y_f), after traversing the AWG, is given by the following expression:

$$\Omega_{AWG,\nu_l}(x_f,y_f,t) = \frac{e^{-i2\pi\nu_l t}}{\sqrt{M+1}}\left\{\Omega(x_f,y_f) + \sum_{k=1}^{M/2}[\Omega_{+k}(x_f,y_f,\nu_l) + \Omega_{-k}(x_f,y_f,\nu_l)]\right\}. \tag{49}$$

With $\Omega_{\pm k}$ and Ω given by (39) and (19), respectively. When photons with different energies are passing simultaneously through the AWG, the probability amplitude density Ω_{AWG} of collecting a photon at the time t in the point (x_f, y_f) after traversing the AWG can be found by superposing the probability amplitude densities corresponding to different photon energies, i.e.,:

$$\Omega_{AWG}(x_f,y_f,t) = \frac{1}{\sqrt{Q+1}}\sum_{l=-Q/2}^{Q/2}\Omega_{AWG,\nu_l}(x_f,y_f,t). \tag{50}$$

Expression (50) can be rewritten in the following, more useful, form:

$$\Omega_{AWG}(x_f,y_f,t) = C\Omega(x_f,y_f)g_{AWG}(y_f,t)e^{-i2\pi\nu_o t}, \tag{51}$$

where $C = 1/\sqrt{(Q+1)(M+1)}$ is the normalization constant of Ω_{AWG}, and:

$$g_{AWG}(y_f,t) = \sum_{l=-Q/2}^{Q/2}g(y_f,\sigma_l)e^{-i2\pi\sigma_l t}. \tag{52}$$

With [see expressions (29) and (40)]

$$g(y_f,\sigma_l) = \sin[(M+1)\alpha_{\nu_l}]/\sin\alpha_{\nu_l}. \tag{53}$$

As shown in expression (34), when a grating or AWG is illuminated with a single monochromatic wave, the temporal dependence of $\Omega_{g\nu}$ is given by the trivial factor $e^{-2\pi\nu t}$. This trivial time dependence results in the time independence of $|\Omega_{g\nu}|^2$ and thus, in a stationary diffraction pattern. However, expressions (51) and (52) show that when an AWG is illuminated with enough short pulses of light, a nontrivial temporal dependence given by the function $g_{AWG}(y_f,t)$ is present in addition to the trivial factor $e^{-2\pi\nu_o t}$. The probability of registering a click at the focal plane in a position with $y = y_f$ at the time t is proportional to $|g_{AWG}(y_f,t)|^2$; thus, the probability distribution of clicks is not stationary when the AWG is illuminated with short pulses of light. When $1/q \ll 1$, the sum given by (52) can be approximated by the integral:

$$g_{AWG}(y_f,t) = \int g(y_f,\sigma_l)e^{-i2\pi\sigma_l t}d\sigma_l. \tag{54}$$

Expression (54) shows that there is a temporal Fourier-transform relationship between the functions $g_{AWG}(y_f,t)$ and $g(y_f,\sigma_l)$. Figure 5 shows two plots of $g(y_f=\text{constant},\sigma_l)$ evaluated for the same parameter-values used in Sec. V and using two different values of y_f (top plot, $y_f=0$, and bottom plot, $y_f=\lambda f/2a$). These values of y_f correspond to the positions marked A and B in the inset in Fig. 4. Several local maxima, spectrally separated by $\Delta\sigma_l = FSR = 50$ GHz, are clearly observed in both plots. The function $g(y_f = \text{constant},\sigma_l)$ has a periodical sequence of local maxima; thus, $g_{AWG}(y_f = \text{constant},t)$ must have several local maxima
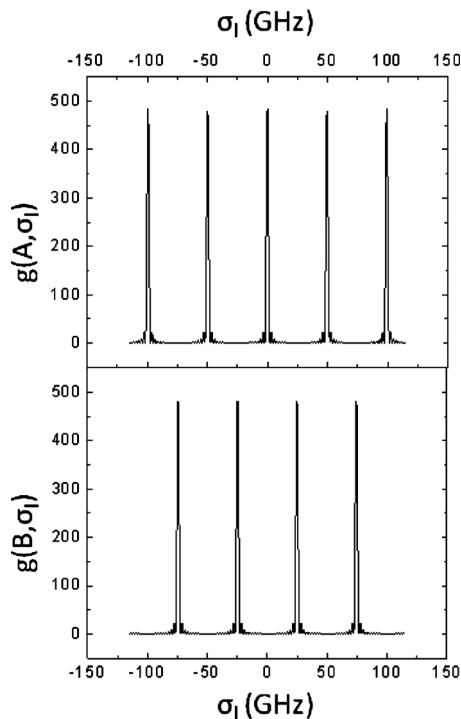
FIG. 5. Calculated values of $g(y_f, \sigma_l)$ for (a) $y_f = 0$ (position A, top plot) and (b) $y_f = \lambda f/2a$ (position B, bottom plot).

separated temporally by $\Delta t = 1/FSR \sim 20$ ps due to the Fourier-transform relationship (54). These temporally periodic local maxima correspond to the pulse-replicas discussed above. This theoretical result is in agreement with experimental results obtained by measuring the temporal response at a particular output waveguide of an specially designed AWG with a free-space autocorrelation apparatus.[5,6,11] In that reference, the autocorrelation apparatus was coupled to an output waveguide. This could neither change the number nor the energy of the photons arriving at the output waveguide. In this way it is possible to know, without altering the experimental conditions of the original experiment,[25] which slab waveguide photons pass through. Nevertheless, interference occurs, and, in accordance with experimental results,[5,6,11] the energies of the photons collected in the output waveguide placed at $y_f = 0$ are different from the energies of the photons collected at the waveguide placed at $y_f = \lambda f/2a$. This statement is supported by the spectral shift in $FSR/2 = 25$ GHz which is clearly visible when comparing the two plots shown in Fig. 5. At $y_f = 0$ (top plot in Fig. 5) the contribution of the frequencies such that $g(y_f = 0, \sigma_l) = 0$ to the sum (52) is zero. That is, photons with the following energies:

$$E_B = h\nu_l, \quad \nu_l \sim \nu_o + (2l - 1)\frac{FSR}{2},$$

$$l = \pm 1, \ldots, \pm Q/2, \tag{55}$$

do not arrive at the output waveguide coupled to spectrometer A. In contrast, at $y_f = \lambda f/2a$ (bottom plot in Fig. 5) the contribution of the frequencies such that $g(y_f = \lambda f/2a, \sigma_l) = 0$ to the sum (52) is zero. This means that photons with the following energies:

$$E_A = h\nu_l, \quad \nu_l \sim \nu_o + l\frac{FSR}{2}, \quad l = 0, \pm 1, \ldots, \pm Q/2, \tag{56}$$

do not arrive at the output waveguide coupled to spectrometer B. Thus, spectrometer A does not register the arrival of photons with energies E_B while the spectrometer B does not register the arrival of photons with energies E_A. That is, interference results in photons with a definite energy arriving only at specific output waveguides. This is an unequivocal signature of interference. It is worth noting that interference would not be recognized if spectrometers A and B were replaced with photodetectors. Due to the broad spectrum of the input pulse, spatial interference maxima corresponding to some frequencies camouflage spatial interference minima corresponding to other frequencies. As a consequence, the number of photons arriving at any output waveguide is approximately equal but their energies are different in distinct waveguides. Thus, the distribution of photodetector clicks at the focal plane of the arrangement shown in Fig. 3 would not have the spatial features used to identify the occurrence of interference. This does not mean that interference has not occurred. This only means that the common method used to recognize the occurrence of interference, in experiments with monochromatic or narrow band feeble light,[23–26] is not appropriate for experiments using a broad band source of light.

In order to understand the peculiarities associated with interference experiments with short pulses of light, it is useful to compare the output response of the same AWG to narrow and broad band light. The broad or narrow character of the light should be defined with respect to the FSR of the AWG. Output spectra taken at any output waveguide have a single peak when the AWG is illuminated with narrow band light ($\Delta\nu < FSR$); however, there are multiple peaks in the spectra when the AWG is illuminated with short pulses of light having $\Delta\nu > FSR$ (broad band illumination).[4–6] In any case, observation of a spectral shift between peaks in the output spectra taken at different output waveguides is a signature of interference. In addition, it should be noted that the external spectrometer used to measure the spectra is not the reason why interference arises in the experimental arrangement. This can be confirmed by obstructing all the slab waveguides of the AWG except one without introducing any other change in the experimental arrangement. After doing that, the output spectra measured using the same spectrometer will not have the characteristics features of interference, i.e., no spectral shift will be observed comparing spectra taken at distinct output waveguides. In other words, photons with different energies are collected at distinct output waveguides when all the slabs waveguides are open. This happens if a spectrometer is coupled to each output waveguide. This also happens if a free-space autocorrelation apparatus is coupled to each output waveguide. When $\Delta\nu < FSR$, spectra taken at any output waveguide have, at most, a peak; thus, as discussed in Sec. VI, the temporal signal arriving at the spectrometer is a single, long, and featureless pulse. For this reason, it is not possible to determine, using a free-space auto-correlation apparatus, which slab waveguide photons passed through to reach the external spectrometer.

The situation is totally different when $\Delta\nu > FSR$. Under broad band illumination, spectra taken at any output waveguide have periodically spaced peaks;[5,6] thus, their Fourier transform corresponds to a pulsed optical signal coming out from the AWG and arriving at the external spectrometer. That is, the information that photons came out of the AWG in packets can be extracted directly from the measured spectra. Alternatively, the which-path information can be obtained by substituting the spectrometer with a free-space autocorrelation apparatus that does not alter the experimental conditions of the original experiment.[5,6]

Summarizing this section, the common saying about the relation between interference and which-path information is only justified in the context of interference experiments using monochromatic or narrow band light. This is the expected situation in experiments with feeble light or single photons. However, one has to be careful when applying it to experiments with ultra short pulses of light. In general, interference features may be either spatial fringes or spectral peaks. These features depend on the measurement instruments (photodetectors or spectrometers) used to identify the occurrence of interference. In experiments with ultra short pulses, where it is possible to find out which path each photon took by time of flight considerations, spatial interference features may be smeared out while spectral interference features are still detectable. In these experiments, the correct predictor of the occurrence of interference is not the impossibility to determine the path of the photons. For instance, it is certain that the first photon arriving at a particular output waveguide in the experiments described in Refs. 5 and 6 was one that traversed through the shortest waveguide of the AWG. In those experiments, the fact that the probability distribution of clicks is not stationary allows one to obtain the which-path information without destroying the interference. The interference of $M+1$ probability amplitudes $\Omega_{\pm k}(x_f, y_f, \nu_l)$, corresponding to photons with the same energy passing through different slab waveguides, results in the collection of equally energetic photons only at specific output waveguides (spatial interference). The interference of $Q+1$ probability amplitudes, corresponding to photons with different energies passing through the same slab waveguide, results in the collection of photons at specific time intervals (time or spectral interference[27]).

VIII. UNCERTAINTY PRINCIPLE AND WHICH-PATH INFORMATION

Heisenberg stated the uncertainty principle originally as follows:[16]

$$\Delta x \Delta p > h. \tag{57}$$

That is, the uncertainties in the position and momentum of a photon at any instant must have their product greater than the Plank's constant. The wide-held belief regarding the relation between interference and which-path information discussed in this work is considered to be a more general statement of the uncertainty principle.[16] However, this wide-held belief can be misleading in interference experiments with ultra short pulses of light. As discussed above in Sec. VII, the enunciate of the common saying regarding the relation between interference and which-path information is correct only if the phrase "perfect interference pattern" means the appearance of spatial interference features in the data collected using photodetectors. In the experiments described in Refs. 5 and 6 where the which-path information was available, interference occurred before light arrived at the external spectrometer used to register the output spectra.[11] This does not violate the uncertainty principle as stated by Heisenberg. To see that this is the case, one can follow Feynman's reasoning to demonstrate that "in order that we shall have a sharp line in our spectrum corresponding to a definite momentum, with an uncertainty given by Δp, we have to have a wave train of at least length $\Delta x = h/\Delta p$.[16]" Feynman discussed the case of a grating illuminated with narrow-band light. In this case, the spectrum has a single narrow peak of width $\Delta\lambda$. This means that the light arriving at the grating was a single featureless long pulse. The peak is produced by interference because the absence of temporal features in the long pulse of light arriving at the spectrometer makes it impossible to obtain the which-path information through time of flight measurements. In contrast to what happens in the narrow band illumination case, a train of pulses arrived to the external spectrometer in the experiments described in Refs. 5 and 6. A train of pulses was characterized by three temporal parameters: the pulse width $\Delta\tau \sim 0.5$ ps, the interval between pulses $\Delta t \sim 20$ ps, and the total duration of the train $\Delta t_T > (M+1)\Delta t$. The duration of the input pulse determines the maximum precision that a time of flight measurement can have. Thus, the length of the optical path of a photon can be determined by using a free-space auto-correlation apparatus with a precision of:

$$\Delta x \sim c\Delta\tau = \frac{c}{\Delta\nu}. \tag{58}$$

That is 150 μm, much smaller than the path length difference of $\Delta L = 4$ mm corresponding to photons traversing consecutive waveguides in the grating of the specially designed AWG. Consequently, which-path information was available in those experiments. In correspondence with the Fourier transform relationship between a temporal signal and its spectrum, the spectrum measured at any output waveguide in those experiments contains numerous peaks that are periodically spaced. The period of the multiple-peaked spectrum is $\sim 1/\Delta t \sim 50$ GHz. The sizes of the smallest features in the spectrum are determined by the size of the longest feature in the temporal signal, which is the total duration of the train (Δt_T). Thus, the width of the peaks in the spectrum is $\Delta\nu_p \sim 1/\Delta t_T < 25$ GHz. The size of the largest feature in the spectrum is determined by the sizes of the shortest features in the temporal signal; thus, the width of the envelope of the peaks in the spectrum is equal to the spectral width of the input pulse. In contrast with what happens in the narrow band case, the width of the narrow peaks in the spectrum does not determine the uncertainties in the measurement of the photon momentum in the broad band illumination case. Certainly, if there was a single peak of width $\Delta\nu_p$ in the spectrum, a featureless pulse of length $\sim c\Delta t_T > \Delta L$ would arrive at the spectrometer. This would make it impossible to find out which waveguide of the grating a photon passed

through. However, photons with various energy ($E=h\nu$) and momentum ($p=h/\lambda$) values were collected in any output waveguide; thus, the uncertainties in the momentum were larger than the one associated with a single peak. In the broad band case Δp is given by the momentum difference corresponding to the most separated peaks in the spectrum measured at any output waveguide, i.e.,:

$$\Delta p \sim h\left(\frac{1}{\lambda_{\text{max}}} - \frac{1}{\lambda_{\text{min}}}\right) = \frac{h}{c}(\nu_{\text{min}} - \nu_{\text{max}}) \sim -\frac{h}{c}\Delta\nu. \quad (59)$$

Thus, in correspondence with Heisenberg's uncertainty principle, from (58) and (59) follows that $|\Delta x||\Delta p| \sim h$.

IX. CONCLUSIONS

The author presented a comprehensive phenomenological quantum description of the ultrafast response of AWGs illuminated with relatively intense short pulses of light. This was achieved with no more mathematical or conceptual complexities than that required by a classical description. This simple but rigorous and detailed, phenomenological quantum description revealed that, in apparent opposition to wide-held beliefs, especially designed AWGs can be used to produce interference in conditions where it is possible to know through which waveguide of the grating photons passed through. Implications of this result on the current understanding of the uncertainty principle were discussed. The presented approach was based on the phenomenological interpretation of the photon, that is, a photon is what produces a click in a photodetector. This was combined with the application of Feynman's rules for describing interference. The author used the Bohr's correspondence principle to illustrate how quantum theory converges in the limit to the classical description of the interference phenomena.

APPENDIX A

Several useful properties of the *FT* are used in this work. For instance, the function $\text{sinc}(f_\xi)$ is the one-dimensional *FT* of the function $\text{rect}(\xi)$,[19] i.e.,:

$$\text{sinc}(f_\xi) = \frac{\sin(\pi f_\xi)}{\pi f_\xi} = FT[\text{rect}(\xi)] = \int_{-\infty}^{+\infty} \text{rect}(\xi)e^{-i2\pi f_\xi\xi}d\xi, \quad (A1)$$

where

$$\text{rect}(\xi) = \begin{array}{ll} 1 & \text{for } |\xi| \le 1/2 \\ 0 & \text{otherwise.} \end{array} \quad (A2)$$

The similarity property of the FT:[19]

$$\text{If } G(f_\xi) = FT[g(\xi)] \Rightarrow FT[g(\alpha\xi)] = G(f_\xi/\alpha)/|\alpha|, \quad (A3)$$

was used to obtain expression (6), and the shift property of the FT:[19]

$$FT[g(\xi - \xi_o)] = G(f_\xi)e^{-i2\pi\xi_o}, \quad (A4)$$

was used to obtain expressions (25) and (39).

APPENDIX B

Using the relation:[18]

$$\sum_{k=1}^{M/2} e^{+i(2k-1)\alpha} = \frac{e^{iM\alpha} - 1}{e^{i\alpha} - e^{-i\alpha}}. \quad (B1)$$

The expression (27) can be rewritten in the following way:

$$\Sigma(y_f) = 1 + e^{i\alpha}\frac{e^{iM\alpha} - 1}{e^{i\alpha} - e^{-i\alpha}} + e^{-i\alpha}\frac{e^{-iM\alpha} - 1}{e^{-i\alpha} - e^{i\alpha}}$$

$$= \frac{\sin[(M+1)\alpha]}{\sin\alpha}. \quad (B2)$$

[1] K. Okamoto, *Fundamentals of Optical Waveguides* (Academic, New York, 2000).
[2] T. Morioka, K. Uchiyama, S. Susuki, and M. Saruwatari, Electron. Lett. **31**, 1064 (1995).
[3] I. Y. Khrushchev, J. D. Bainbridge, J. E. A. Whiteway, I. H. White, and R. V. Petty, IEEE Photonics Technol. Lett. **11**, 1659 (1999).
[4] D. E. Leaird, S. Shen, A. M. Weiner, A. Sigita, S. Kamei, M. Ishii, and K. Okamoto, IEEE Photonics Technol. Lett. **13**, 221 (2001).
[5] L. Grave de Peralta, A. A. Bernussi, and H. Temkin, IEEE J. Quantum Electron. **43**, 473 (2007).
[6] L. Grave de Peralta, A. A. Bernussi, and H. Temkin, J. Lightwave Technol. **25**, 2410 (2007).
[7] M. Smit, Electron. Lett. **24**, 385 (1988).
[8] C. Dragone, C. A. Edwards, and R. C. Kistler, IEEE Photonics Technol. Lett. **3**, 896 (1991).
[9] L. Grave de Peralta, A. A. Bernussi, S. Frisbie, R. Gale, and H. Temkin, IEEE Photonics Technol. Lett. **15**, 1398 (2003).
[10] P. J. Bock, P. Cheben, J. H. Schmid, A. Delâge, D. X. Xu, S. Janz, and T. J. Hall, Opt. Express **17**, 19120 (2009).
[11] L. Grave de Peralta, J. Appl. Phys. **105**, 013111 (2009).
[12] B. L. Van Der Waerden, in *Sources of Quantum Mechanics*, edited by G. Holton (Dover, New York, 1967).
[13] M. O. Scully and M. S. Zubairy, *Quantum Optics* (Cambridge University Press, Cambridge, 1997).
[14] R. P. Feynman and A. R. Hibbs, *Quantum Mechanics and Path Integrals* (MacGraw-Hill, New York, 1965).
[15] B. J. Smith and M. G. Raymer, New J. Phys. **9**, 414 (2007).
[16] R. P. Feynman, R. B. Leighton, and M. Sands, *The Feynman Lectures on Physics* (Addison-Wesley, Massachusetts, 1965), Vol. II.
[17] A. Zeilinger, G. Weihs, T. Jennewein, and M. Asppeimeyer, Nature (London) **433**, 230 (2005).
[18] F. L. Pedrotti, L. S. Pedrotti, and L. M. Pedrotti, *Introduction to Optics*, 3rd ed. (Pearson Prentice Hall, New Jersey, 2007).
[19] J. W. Goodman, *Introduction to Fourier Optics* (McGraw-Hill, New York, 1968).
[20] P. R. Holland, *The Quantum Theory of Motion* (Cambridge University Press, Cambridge, 1993).
[21] P. A. M. Dirac, *The Principles of Quantum Mechanics*, 4th ed. (Clarendon, Oxford, 1958).
[22] R. J. Glauber, Am. J. Phys. **63**, 12 (1995).
[23] S. P. Walborn, M. O. Terra Cunha, S. Pádua, and C. H. Monken, Phys. Rev. A **65**, 033818 (2002).
[24] G. Brida, E. Cagliero, G. Falzetta, M. Genovese, and M. Gramegna, Phys. Rev. A **68**, 033803 (2003).
[25] L. Mandel, Rev. Mod. Phys. **71**, S274 (1999).
[26] Y. Kim, M. V. Chekhova, S. P. Kulik, and Y. Shih, Phys. Rev. A **60**, R37 (1999).
[27] S. L. Chin, V. Francois, J. M. Watson, and C. Delisle, Appl. Opt. **31**, 3383 (1992).